NMR spectra of phenyl derivatives.[63] In the planar form, the C1-C5 distance is approximately 2.5 Å, and the π interaction between the ends of the dienylic system is negligible. Puckering may increase overlap by virtue of the accompanying canting of the C1,C5 p-orbitals toward one another, but it does so only at the expense of a favorable π-interaction between the dienylic HOMO and the $\pi^*(CH_2)$ fragment orbital at C6. Thus, mo-

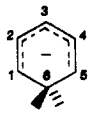

16

nohomoconjugation in this carbanion is unimportant. Interestingly, the C2-C7 and C4-C6 distances in ion **2** are also on the order of 2.5 Å,[11,12] yet bishomoconjugative interactions are evident. The key difference is that the rigid, bicyclic framework in **2** effects a canting of the two π-systems toward one another on the endo face of the molecule in such a way that good overlap can be achieved. The apparent stabilization exhibited by homoaromatic dianion **6**[16] also serves to illustrate this geometric criterion, since it has been shown recently that the potentially monohomoconjugated planar analogue **22** is, in fact, substantially *destabilized* relative to cyclooctatetraenyl dianion.[64] In view of this trend,

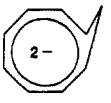

22

it is useful to envisage other compounds which might possess similar structural features as **2** and **6**. An excellent candidate for "tetrakishomoaromaticity" is carbanion **23**, the conjugate base of dicyclopentadiene. Simple models show that the C3-C9 and C5-C8 distances are nearly the same as the C2-C7 and C4-C6

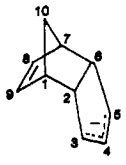

23a

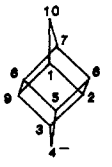

23b

(63) Tolbert, L. M.; Rajca, A. *J. Org. Chem.* **1985**, *50*, 4805.
(64) Concepcion, R.; Reiter, R. C.; Stevenson, G. R. *J. Am. Chem. Soc.* **1983**, *105*, 1778.

in **2** but, more importantly, that the p-orbitals in the allylic and olefinic fragments are oriented almost directly at one another, with nearly perfect σ symmetry. We are presently attempting to generate carbanion **23** in the gas phase by proton abstraction from dicyclopentadiene, although its low volatility possesses somewhat of a practical problem for flowing afterglow experiments. In this context, it is interesting to note that one of the canonical forms for a fully delocalized tetrakishomoaromatic ion **23** corresponds to bishomocubyl anion **23b**. Thus, proton abstraction from bishomocubane may provide an alternate entry to **23**.

Conclusion

Bishomoaromaticity in the conjugate base carbanion is the main cause of the unusually high gas-phase acidity of bicyclo[3.2.1]-octa-2,6-diene. Of the total 9.5 kcal/mol measured acidity enhancement relative to bicyclo[3.2.1]oct-2-ene, roughly a third of this amount can be attributed to field/inductive effects of the remote C6-C7 double bond, as modelled by the 3.1 kcal/mol acidity increase measured for norbornadiene over norbornene. The polarizability difference between these two hydrocarbons makes a negligible contribution, while angle strain in the allylic bridge of **3** reduces its acidity by approximately 3 kcal/mol. We must conclude from our results that the failure to detect bishomoconjugative interactions in **2** in the earlier theoretical studies[11,12] was an artifact of the inadequacies of the basis sets and the molecular geometries which were employed. At the time of these studies, adoption of a lower level of theory to examine the problem was dictated by the large size of the bicyclic alkenes and carbanions involved. Given the computational advances that have become available since then, it would seem that a reexamination is warranted. We anticipate that calculation of the electronic and geometric structures of **2** with use of basis sets which are properly augmented with diffuse functions[15] will expose the sought-after homoaromatic interactions.

Acknowledgment. We are most grateful to Professors Grutzner, Jorgensen, Schleyer, and Chandrasekhar for many helpful and stimulating discussions on this problem. Dr. Pirjo Vainiotalo is gratefully acknowledged for providing us with samples of 2-methylenenorbornane. We also thank the donors of the Petroleum Research Fund, administered by the American Chemical Society, Research Corporation, and the National Science Foundation (CHE-8502515) for their support of this research.

Gas-Phase Photodissociation of Organometallic Ions: Bond Energy and Structure Determinations

R. L. Hettich, T. C. Jackson, E. M. Stanko, and B. S. Freiser*

Contribution from the Department of Chemistry, Purdue University, West Lafayette, Indiana 47907. *Received December 20, 1985*

Abstract: The photodissociation of a variety of gas-phase organometallic ions was investigated with Fourier transform mass spectrometry in order to obtain spectroscopic and thermodynamic information on these complexes. The results indicate that these ionic complexes absorb broadly and photodissociate readily in the ultraviolet and visible spectral regions, with cross sections for λ_{max} ranging from 0.02 to 0.30 Å^2. Because of this broad absorption, photodissociation thresholds are attributed to thermodynamic and not spectroscopic factors. Bond energies and heats of formation obtained by monitoring photodissociation onsets show good agreement with those obtained by other techniques. Interestingly, product ions generated by photodissociation are found to differ significantly in a number of instances from those produced by collision-induced dissociation. Finally, differentiation of two $FeC_4H_6^+$ and four $NiC_4H_8^+$ isomers is demonstrated by observing differences in cross sections, spectral band positions, and neutral losses.

Gas-phase organometallic ion chemistry has become an active area in recent years with the arsenal of experimental techniques employed constantly growing.[1-4] Delineating reaction mechanisms has been a major focus, drawing heavily on results from exper-

0002-7863/86/1508-5086$01.50/0

iments which probe product ion structure and thermochemistry. Knowing the structure or structures of the final products is clearly important in formulating mechanisms, and likewise, having thermochemical information on metal–ligand bond making and bond breaking is required to determine whether a mechanism is energetically feasible. For both types of determinations, it is desirable to use a variety of complementary techniques as a cross-check of the results. Among the structural probes, collision-induced dissociation (CID)[5] and selective ion–molecule reactions[6] are two of the most widely used techniques. A great deal of useful thermodynamic information has been obtained from monitoring the thresholds of endothermic reactions,[7] from observation of exothermic reactions,[8] and from equilibrium ligand-exchange reactions.[9]

A parallel development has been taking place in the area of gas-phase ion photochemistry.[10] The number of instruments and techniques being applied has multiplied, with large bodies of results now available from ion beams,[11] drift tubes,[12] tandem quadrupoles,[13] radio frequency quadrupole traps,[14] and ion cyclotron resonance (ICR) instruments.[15] In particular, photodissociation experiments have been shown to yield information about ion excited states, ion structure, and ion thermochemistry.[10] While the field is well developed for organic ions,[16] still relatively few studies on metal ion containing systems have been reported.[17] These early studies along with the results presented here on the photodissociation of a variety of transition-metal ligand ions in the gas phase suggest that this will be a particularly fruitful area to pursue.

Experimental Section

The theory and instrumentation of Fourier transform mass spectrometry (FTMS) have been discussed elsewhere.[18] All experiments were performed on a Nicolet prototype FTMS-1000 Fourier transform mass spectrometer previously described in detail[19] and equipped with a 5.2-cm cubic trapping cell situated between the poles of a Varian 15-in. electromagnet maintained at 0.85 T. The cell was constructed in our laboratory and in this study utilized two 80% transmittance stainless steel screens as the transmitter plates. This permitted irradiation with a 2.5 kW Hg–Xe arc lamp, used in conjunction with a Schoeffel 0.25-m monochromator set for 10-nm resolution. Metal ions were generated by focusing the beam of a Quanta Ray Nd:YAG laser (either the fundamental line at 1064 nm or the frequency doubled line at 532 nm) into the center-drilled hole (1 mm) of a high-purity rod of the appropriate metal supported on the transmitter screen nearest to the laser. The laser ionization technique for generating metal ions has been outlined elsewhere.[20]

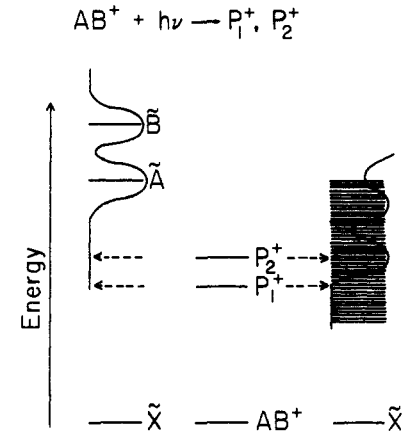

Figure 1. An energy level diagram depicting cases where photodissociation thresholds are determined by spectroscopic factors (left side) and thermodynamic factors (right side).

Details of the collision-induced dissociation (CID) experiments have been described.[21] Argon was used as the collision gas at a total pressure of $\sim 4 \times 10^{-6}$ Torr. The collision energy of the ions can be varied (typically between 0 and 100 eV). A Bayard-Alpert ionization gauge was used to monitor static pressures.

Each of the chemicals used was obtained commercially, except for the (trimethylenemethane)iron tricarbonyl which was synthesized in Professor R. Squires' laboratory at Purdue,[22] and was used without further purification, except for multiple freeze–pump–thaw cycles to remove noncondensible gases. Electron impact mass spectrometry indicated no detectable impurities. All samples were admitted to the cell through a General Valve Corp. Series 9 pulsed solenoid valve.[23] The pulsed valve, which was triggered concurrently with the laser pulse used to generate the metal ions, introduced the reagent gas into the vacuum chamber to a maximum pressure of approximately 10^{-5} Torr. Although the pulse duration of the valve was 2 ms, the pressure of the reagent gas had a rise time of about 200 ms and was pumped away by a high-speed 5-in. diffusion pump in approximately 400 ms. Swept double resonance pulses were then used to isolate the ion of interest, which was subsequently trapped for 3–6 s (determined by the ion's cross section for photodissociation) in either the presence or absence of radiation. For each ion, two sets of photodissociation spectra were taken, one at 2×10^{-6} Torr (argon), to permit collisional cooling, and another in a background pressure of $\sim 10^{-8}$ Torr.[24] In all cases, data from the collisionally cooled ions are presented.

Photodissociation spectra were obtained by monitoring the appearance of ionic photoproducts as a function of the wavelength of light. Shot-to-shot variation of the laser generated metal precursor ions made monitoring the photodisappearance of the parent ions impractical. Assuming a one-photon process,[25] the photodissociation of AB^+, eq 1, can be described by first-order kinetics, eq 2, where σ_A and σ_B are the absolute

(1) (a) Armentrout, P. B.; Loh, S. K.; Ervin, K. M. *J. Am. Chem. Soc.* **1984**, *106*, 1161. (b) Houriet, R.; Halle, L. F.; Beauchamp, J. L. *Organometallics* **1983**, *2*, 1818.
(2) (a) Allison, J.; Radecki, B. *J. Am. Chem. Soc.* **1984**, *106*, 946. (b) Larsen, B. S.; Ridge, D. P. *J. Am. Chem. Soc.* **1984**, *106*, 1912.
(3) (a) Jacobson, D. B.; Freiser, B. S. *J. Am. Chem. Soc.* **1985**, *107*, 1581. (b) Morse, M. D.; Smalley, R. E. *Ber. Bunsenges. Phys. Chem.* **1984**, *88*, 228. (c) Anderson Fredeen, D.; Russel, D. H. *J. Am. Chem. Soc.* **1985**, *107*, 3762.
(4) (a) Lane, K. R.; Sallans, L.; Squires, R. R. *Organometallics* **1985**, *4*, 408. (b) Sanders, L.; Weisshaar, J. C. 33rd Annual Conference on Mass Spectrometry and Allied Topics, San Diego, California, 1985.
(5) (a) Peake, D. A.; Gross, M. L.; Ridge, D. P. *J. Am. Chem. Soc.* **1984**, *106*, 4307. (b) Jacobson, D. B.; Freiser, B. S. *J. Am. Chem. Soc.* **1983**, *105*, 5197.
(6) Jacobson, D. B.; Freiser, B. S. *J. Am. Chem. Soc.* **1985**, *107*, 72.
(7) Armentrout, P. B.; Halle, L. F.; Beauchamp, J. L. *J. Chem. Phys.* **1982**, *76*, 2449.
(8) (a) Allison, J.; Ridge, D. P. *J. Am. Chem. Soc.* **1979**, *101*, 4998. (b) Jacobson, D. B.; Freiser, B. S. *J. Am. Chem. Soc.* **1983**, *105*, 7492.
(9) Uppal, J. S.; Staley, R. H. *J. Am. Chem. Soc.* **1982**, *104*, 1229.
(10) Dunbar, R. C. *Gas Phase Ion Chemistry*; Bowers, M. T., Ed.; Academic Press, Inc.: New York, 1984; Vol. 3, Chapter 20.
(11) (a) Mukhtar, E. S.; Griffiths, I. W.; Harris, F. M.; Beynon, J. H. *Int. J. Mass Spectrom. Ion Phys.* **1981**, *37*, 159. (b) Carrington, A.; Milverton, D. R. J.; Sarre, P. J. *Mol. Phys.* **1976**, *32*, 297.
(12) (a) Zwier, T. S.; Bierbaum, V. M.; Ellison, G. B.; Leone, S. R. *J. Chem. Phys.* **1980**, *72*, 5426. (b) Hamilton, C. E.; Duncan, M. A.; Zwier, T. S.; Weisshaar, J. C.; Ellison, G. B.; Bierbaum, V. M.; Leone, S. R. *Chem. Phys. Lett.* **1983**, *94*, 4.
(13) (a) Vestal, M. L.; Futrell, J. H. *Chem. Phys. Lett.* **1974**, *28*, 559. (b) Vestal, M. L.; Mauclaire, G. H. *J. Chem. Phys.* **1977**, *67*, 3758.
(14) Ensberg, E. S.; Jefferts, K. B. *Astrophys. J.* **1975**, *195*, L89.
(15) (a) Dunbar, R. C. *Mass Spectrometry*; Johnston, R. A. W., Ed.; The Royal Society: London, 1981; Vol. 6, p 100. (b) Wright, C. A.; Beauchamp, J. L. *J. Am. Chem. Soc.* **1981**, *103*, 6449.
(16) (a) Woodin, R. L.; Bomse, D. S.; Beauchamp, J. L. *J. Am. Chem. Soc.* **1978**, *100*, 3248. (b) Morgenthaler, L. N.; Eyler, J. R. *Int. J. Mass Spectrom. Ion Phys.* **1981**, *37*, 153. (c) Moylan, C. R.; Jasinski, J. M.; Brauman, J. I. *J. Am. Chem. Soc.* **1985**, *107*, 1934. (d) Hanovich, J. P.; Dunbar, R. C.; Lehman, T. *J. Phys. Chem.* **1985**, *89*, 2513.
(17) (a) Dunbar, R. C.; Hutchinson, B. B. *J. Am. Chem. Soc.* **1974**, *96*, 3816. (b) Freiser, B. S.; Staley, R. H.; Beauchamp, J. L. *Chem. Phys. Lett.* **1976**, *39*, 49. (c) Burnier, R. C.; Freiser, B. S. *Inorg. Chem.* **1979**, *18*, 906. (d) Cassady, C. J.; Freiser, B. S. *J. Am. Chem. Soc.* **1984**, *106*, 6176.
(18) Comisarow, M. B. *Adv. Mass Spectrom.* **1980**, *8*, 1698.
(19) Cody, R. B.; Burnier, R. C.; Freiser, B. S. *Anal. Chem.* **1982**, *54*, 96.
(20) Burnier, R. C.; Byrd, G. D.; Freiser, B. S. *J. Am. Chem. Soc.* **1981**, *103*, 4360.
(21) Burnier, R. C.; Cody, R. B.; Freiser, B. S. *J. Am. Chem. Soc.* **1982**, *104*, 7436.
(22) The (trimethylenemethane)iron tricarbonyl was synthesized from $Fe_2(CO)_9$ and 3-chloro-2-chloromethylpropene as outlined in the following: Ehrlich, K.; Emerson, G. F. *J. Am. Chem. Soc.* **1972**, *94*, 2464. Proton NMR of the $Fe(C_4H_6)(CO)_3$ revealed six equivalent protons.
(23) Carlin, T. J.; Freiser, B. S. *Anal. Chem.* **1983**, *55*, 571.
(24) The photodissociation spectra of all of the ions showed no pressure dependence, except for slight quenching of the low energy tail region, indicating that photodissociation in these cases is probably due to one-photon excitation.
(25) For discussion of multiple-photon dissociation, see: Freiser, B. S.; Beauchamp, J. L. *Chem. Phys. Lett.* **1975**, *35*, 35.

$$AB^+ + h\nu \rightarrow A^+ \quad \rightarrow B^+ \qquad (1)$$

cross sections for production of the photoproducts A^+ and B^+, respectively, and I is the photon flux. Integrating eq 2 and substituting $(AB^+)_0$

$$d(AB^+)/dt = -(\sigma_A + \sigma_B)I(AB^+) \qquad (2)$$

$= (AB^+)_{h\nu} + (A^+)_{h\nu} + (B^+)_{h\nu}$ relates the extent of photodissociation to the cross section at a given wavelength, eq 3, where $\sigma_T = \sigma_A + \sigma_B$ is the total cross section and t is the irradiation time. Solving eq 3 for σ_T and

$$\ln\left[1 + \frac{A^+ + B^+}{AB^+}\right] = \sigma_T It \qquad (3)$$

plotting that value as a function of wavelength, appropriately correcting for the blanks (no light), yields the photodissociation spectrum of the ion (i.e., relative σ_T vs. wavelength). Photoappearance curves for the individual photoproducts can be obtained, for example, by solving eq 4 for σ_A and plotting it as a function of wavelength. Each spectrum reported

$$\left[\frac{A^+}{A^+ + B^+}\right]\ln\left[1 + \frac{A^+ + B^+}{AB^+}\right] = \sigma_A It \qquad (4)$$

is an average of several trials. The reproducibility of the peak intensities is ±40% and that of the peak locations is ±10 nm. Photodissociation thresholds were confirmed by using cutoff filters.

To obtain absolute values for the cross sections of the ions being examined, the photodissociation of $C_7H_8^+$ (from toluene at 20 eV) at 410 nm (σ (410 nm) = 0.05 Å^2)[26] was compared to the photodissociation of a given ion at its λ_{max}, both taken under similar experimental conditions. All cross sections determined in this manner have an estimated uncertainty of ±50% due to instrumental variables.

Results and Discussion

In order to observe photodissociation, process 5, three criteria

$$AB^+ + h\nu \rightarrow P_1^+ \quad [\Delta H_f^\circ(P_1^+) < \Delta H_f^\circ(P_2^+)] \quad \rightarrow P_2^+ \qquad (5)$$

must be satisfied; first, the ion AB^+ must absorb a photon; second, the photon energy must exceed the positive enthalpy required to generate the products (assuming a one-photon process); and third, the quantum yield for photodissociation must be non-zero. If the first allowed electronic state of AB^+ lies at an energy above that required to generate any of the products, as illustrated in Figure 1, the observed photodissociation onset is spectroscopically determined and yields only an upper energy limit for the process(es). If, however, an allowed electronic state fortuitously lies at the same energy as the lowest energy process or, as shown in Figure 1, there is a high density of allowed states having energies in the vicinity of the thermodynamic threshold (i.e., the ion absorbs over a broad wavelength region), the observed photodissociation onset should accurately reflect the dissociation energy for process 5 provided, once again, that there is a sufficient quantum yield under these broad absorption conditions. Onsets for higher energy products will also reflect the thermochemistry if rapid internal conversion to a vibrationally excited ground state occurs randomizing the energy.

An earlier photodissociation study on FeL^+ (L = CO, C_2H_4, and OH)[17d] together with the systems discussed in this paper suggests that many of these metal ion complexes do in fact absorb broadly and that the photoappearance onsets in these cases reflect the thermochemistry. In particular, values obtained by observing photodissociation onsets are found in general to be in good agreement with those obtained by other techniques.

(I) Bond Energy Determinations. (A) MCH_2^+. $FeCH_2^+$ and $CoCH_2^+$ can be generated from ethylene oxide, reaction 6. We have recently reported the photodissociation of these two ions.[27]

$$M^+ + \triangle^{O} \rightarrow MCH_2^+ + CH_2O \qquad (6)$$

(M = Fe, Co)

Interestingly, photodissociation of these ions yields different products than are observed by their collision-induced dissociation. Low-energy CID (<100 eV) of either $FeCH_2^+$ or $CoCH_2^+$ results in exclusive cleavage of CH_2 to regenerate the metal ion. Photodissociation of these metal carbene ions, however, yields three photoproducts: MCH^+, MC^+, and M^+. Several other examples of different products arising from photodissociation and collision-induced dissociation were also observed in this study and are discussed below. By monitoring the photodissociation thresholds for each of the three photoproducts, bond energies for M^+–C, M^+–CH, and M^+–CH_2 were obtained (see Table I).

(B) MCH_3^+. $FeCH_3^+$ and $CoCH_3^+$ were synthesized by reaction 7. A previous study indicated that these MCH_3^+ species

$$M^+ + CH_3I \rightarrow MCH_3^+ + I \qquad (7)$$

(M = Fe, Co)

exist as a methyl bound to the metal and not a hydrido–carbene metal ion (H—M=CH_2^+).[28] Photodissociation provides additional evidence for this since the only photoproduct observed at any energy is M^+, reaction 8. This single photoproduct is surprising in view of the multiple products observed for the corresponding carbene ions. Losses of H and H_2 to generate MCH_2^+ and MCH^+, reactions 9 and 10, are energetically feasible in the ultraviolet region. For M = Fe, reaction 9 should occur out to 304 nm (94 kcal/mol) and reaction 10 should occur out to 390 nm (73 kcal/mol). For M = Co, MCH_2^+ (reaction 9) should be produced out to 340 nm (84 kcal/mol) and MCH^+ should be observed out to 430 nm (66 kcal/mol). One possible explanation why reaction 8 is the only photoprocess observed for MCH_3^+ is that simple cleavage of CH_3 from MCH_3^+ is kinetically favored over the rearrangements required to form MCH_2^+ and MCH^+. Alternatively, excitation directly into a dissociative electronic state is a possibility. Finally, observation of a single photoproduct for MCH_3^+ and multiple photoproducts for MCH_2^+ may also be due to the weaker bond energy of M^+–CH_3 relative to M^+–CH_2.

$$MCH_3^+ + h\nu \rightarrow M^+ + CH_3 \qquad (8)$$

$$MCH_3^+ + h\nu \rightarrow MCH_2^+ + H \qquad (9)$$

$$MCH_3^+ + h\nu \rightarrow MCH^+ + H_2 \qquad (10)$$

Table I. Bond Energy Determinations

A^+–B	$D^\circ(A^+$–B) (kcal/mol) photodissociation	lit.
Co^+–CH_2	84 ± 5[a]	85 ± 7[b]
Co^+–CH	100 ± 5[a]	
Co^+–C	90 ± 5[a]	98[c]
Fe^+–CH_2	82 ± 5[a]	96 ± 5[d]
Fe^+–CH	101 ± 5[a]	115 ± 20[c]
Fe^+–C	94 ± 5[a]	89[c]
Fe^+–CH_3	65 ± 5	69 ± 5[e]
Co^+–CH_3	57 ± 7	61 ± 4[f]
Fe^+–O	68 ± 5	68 ± 3[f]
Fe^+–S	65 ± 5	74 > x > 59[g]
Co^+–S	62 ± 5	74 > x > 59[g]
Ni^+–S	60 ± 5	
V^+–C_6H_6	62 ± 5	
$C_6H_6V^+$–C_6H_6	57 ± 5	
Co^+–C_6H_6	68 ± 5	71 > x > 61[h]
Fe^+–C_6H_6	55 ± 5	59 ± 5[i]
V^+–Fe	75 ± 5[j]	
Ni^+–$2C_2H_4$	80 ± 5	74 ± 2[k]
Ni^+–C_3H_5	<60	≥55[l]
Fe^+–butadiene	48 ± 5	45–60[m]

[a] Reference 27. [b] Armentrout, P. B.; Beauchamp, J. L. *J. Chem. Phys.* **1981**, *74*, 2819. [c] Beauchamp, J. L., private communication. [d] Armentrout, P. B.; Halle, L. F.; Beauchamp, J. L. *J. Am. Chem. Soc.* **1981**, *103*, 6501. [e] Reference 29. [f] Reference 30. [g] Carlin, T. J. Ph. D. Thesis, Purdue University, 1984. [h] Reference 33. [i] Reference 35. [j] Reference 37. [k] Reference 8b. [l] Reference 32. [m] Reference 43.

(26) Dunbar, R. C. *Chem. Phys. Lett.* **1975**, *32*, 508.
(27) Hettich, R. L.; Freiser, B. S. *J. Am. Chem. Soc.* **1986**, *108*, 2537.
(28) Jacobson, D. B.; Freiser, B. S. *J. Am. Chem. Soc.* **1984**, *106*, 3891.

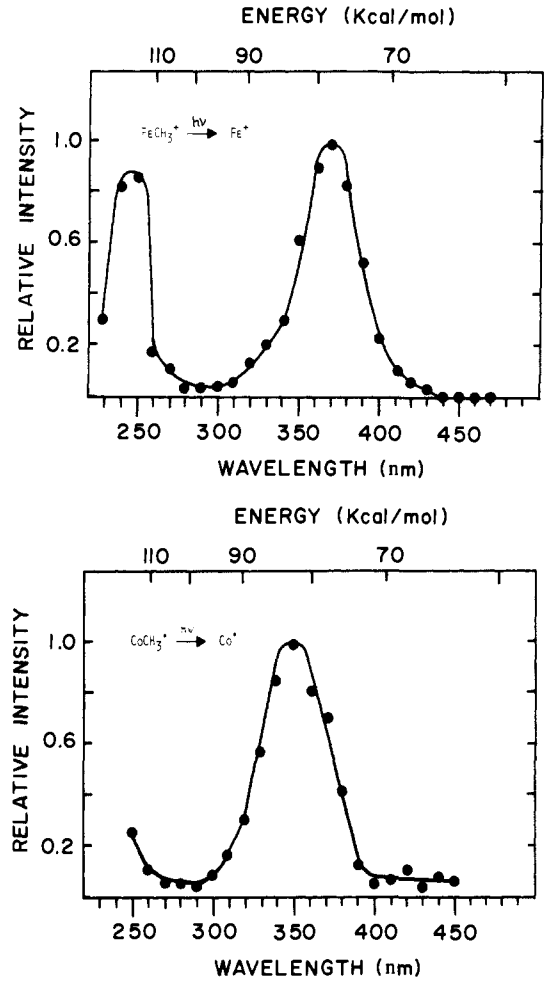

Figure 2. (a) The photodissociation spectrum of $FeCH_3^+$ obtained by monitoring reaction 8 as a function of wavelength. (b) The photodissociation spectrum of $CoCH_3^+$ obtained by monitoring reaction 8 as a function of wavelength.

Spectra a and b in Figure 2 illustrate the photodissociation spectra of $FeCH_3^+$ and $CoCH_3^+$, respectively. Both ions have large cross sections for dissociation: σ(370 nm) = 0.22 Å^2 for $FeCH_3^+$ and σ(350 nm) = 0.21 Å^2 for $CoCH_3^+$. The dissociation thresholds for both metal–methyl ions are difficult to determine because the cutoffs are not sharp. $D°(Fe^+–CH_3) < 70$ kcal/mol is implied since significant dissociation occurs at 410 nm. The threshold at 440 ± 10 nm observed for $FeCH_3^+$ at a static pressure of 2×10^{-6} Torr of argon implies $D°(Fe^+–CH_3) = 65 \pm 5$ kcal/mol, in good agreement with a previously reported value of $D°(Fe^+–CH_3) = 69 \pm 5$ kcal/mol.[29] $CoCH_3^+$ dissociates readily at 390 nm, implying $D°(Co^+–CH_3) < 73$ kcal/mol. $Co^+–CH_3$ does not photodissociate at 540 nm (which is an intense line from the Hg–Xe arc lamp), suggesting $D°(Co^+–CH_3) > 53$ kcal/mol. The featureless, low-energy tail is unaffected by argon pressure and extends out to 500 nm (observed using cutoff filters with white light), implying $D°(Co^+–CH_3) = 57 \pm 7$ kcal/mol. A value of $D°(Co^+–CH_3) = 61 \pm 4$ kcal/mol has been previously determined.[30]

(C) FeO^+. Reaction 11 was used to generate FeO^+ while CoO^+ and NiO^+ could not be produced in sufficient abundances to

$$Fe^+ + N_2O \rightarrow FeO^+ + N_2 \qquad (11)$$

isolate and study. FeO^+ photodissociates, as expected, to give Fe^+ as the only photoproduct. The photodissociation spectrum of FeO^+, shown in Figure 3, has a cross section σ(260 nm) = 0.07 Å^2 and a threshold at 420 ± 10 nm, which implies $D°(Fe^+–O) = 68 \pm 5$ kcal/mol. A previous study by Beauchamp and coworkers yielded $D°(Fe^+–O) = 68 \pm 3$ kcal/mol.[29]

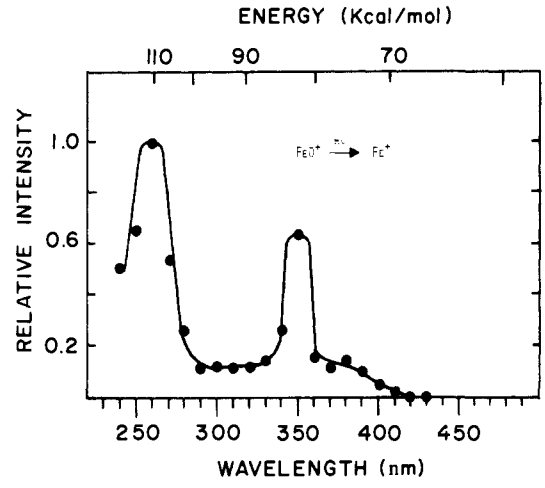

Figure 3. The photodissociation spectrum of FeO^+ obtained by monitoring the appearance of Fe^+ as a function of wavelength.

(D) MS^+. FeS^+ and CoS^+ can be synthesized by reaction 12, implying $D°(M^+–S) > 59$ kcal/mol.[31] NiS^+ can be made according to reaction 13, implying $D°(Ni^+–S) > 54$ kcal/mol. The photodissociation spectra of MS^+ (M = Fe, Co, Ni), shown in Figure 4a–c, all produce M^+ upon irradiation. One major peak at 320 nm (σ = 0.30 Å^2) is observed for FeS^+ (Figure 4a). Surprisingly, the cross section of FeS^+ is about four times larger than that of FeO^+. The threshold at 440 ± 10 nm implies $D°(Fe^+–S) = 65 \pm 5$ kcal/mol.

$$M^+ + \triangle^{S} \longrightarrow MS^+ + C_2H_4 \qquad (12)$$
(M = Fe, Co)

$$Ni^+ + CH_3SH \rightarrow NiS^+ + CH_4 \qquad (13)$$

The photodissociation spectrum of CoS^+ (Figure 4b) shows peaks at 300 nm (σ = 0.09 Å^2) and 390 nm with a threshold at 460 ± 10 nm, implying $D°(Co^+–S) = 62 \pm 5$ kcal/mol. Figure 4c, the photodissociation of NiS^+, also reveals two peaks at 280 nm (σ = 0.10 Å^2) and 420 nm. A threshold is observed at 480 ± 10 nm, implying $D°(Ni^+–S) = 60 \pm 5$ kcal/mol. These $M^+–S$ bond energies are in good agreement with values obtained by ion–molecule reactions.[32]

(E) $M(C_6H_6)^+$ and $M(C_6H_6)_2^+$. Primary and secondary reactions of M^+ (M = V, Fe, Co) with cyclohexene produce $M(C_6H_6)^+$ and $M(C_6H_6)_2^+$, respectively. These reactions imply $D°(M^+–C_6H_6)$ and $D°(C_6H_6M^+–C_6H_6)$ both exceed 30 kcal/mol, which is the energy required to dehydrogenate cyclohexene to benzene.[31]

Both collision-induced dissociation and photodissociation of $M(C_6H_6)^+$ yield M^+ exclusively. The photodissociation spectrum of $VC_6H_6^+$ is shown in Figure 5a. A peak maximum is observed at 300 ± 10 nm (σ = 0.02 Å^2). The threshold for dissociation at 460 ± 10 nm implies $D°(V^+–C_6H_6) = 62 \pm 5$ kcal/mol. $VC_6H_6^+$ can also be made by reacting V^+ with cyclohexane. For this reaction to occur, $D°(V^+–C_6H_6)$ must exceed the 49 kcal/mol required to dehydrogenate cyclohexane to benzene. The photodissociation spectrum of $VC_6H_6^+$ formed from cyclohexane is identical with that shown in Figure 5a from cyclohexene, including the threshold at 460 ± 10 nm. This result indicates that reaction exothermicity does not significantly affect the dissociation threshold in this case, presumably because the ions have had sufficient time to cool.

(29) Halle, L. F.; Armentrout, P. B.; Beauchamp, J. L. *Organomet.* **1982**, *1*, 963.
(30) Armentrout, P. B.; Beauchamp, J. L. *J. Am. Chem. Soc.* **1981**, *103*, 784.
(31) All heats of formation and other supplemental thermodynamic values are taken from Rosenstock et al. (Rosenstock, H. M.; Draxl, K.; Steiner, B. W.; Herron, J. T. *J. Phys. Chem. Ref. Data, Suppl. 1* **1977**, 6).
(32) Jackson, T. C.; Freiser, B. S. *Int. J. Mass Spectrom. Ion Phys.*, in press.

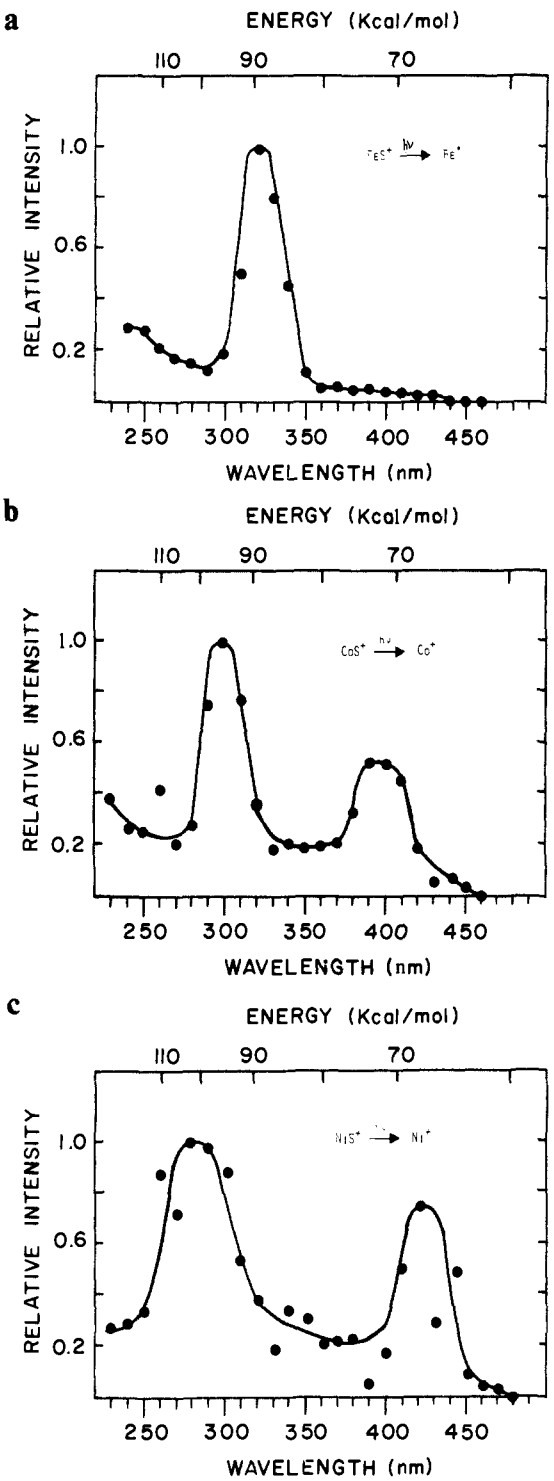

Figure 4. (a) The photodissociation spectrum of FeS^+ obtained by monitoring the appearance of Fe^+ as a function of wavelength. (b) The photodissociation spectrum of CoS^+ obtained by monitoring the appearance of Co^+ as a function of wavelength. (c) The photodissociation spectrum of NiS^+ obtained by monitoring the appearance of Ni^+ as a function of wavelength.

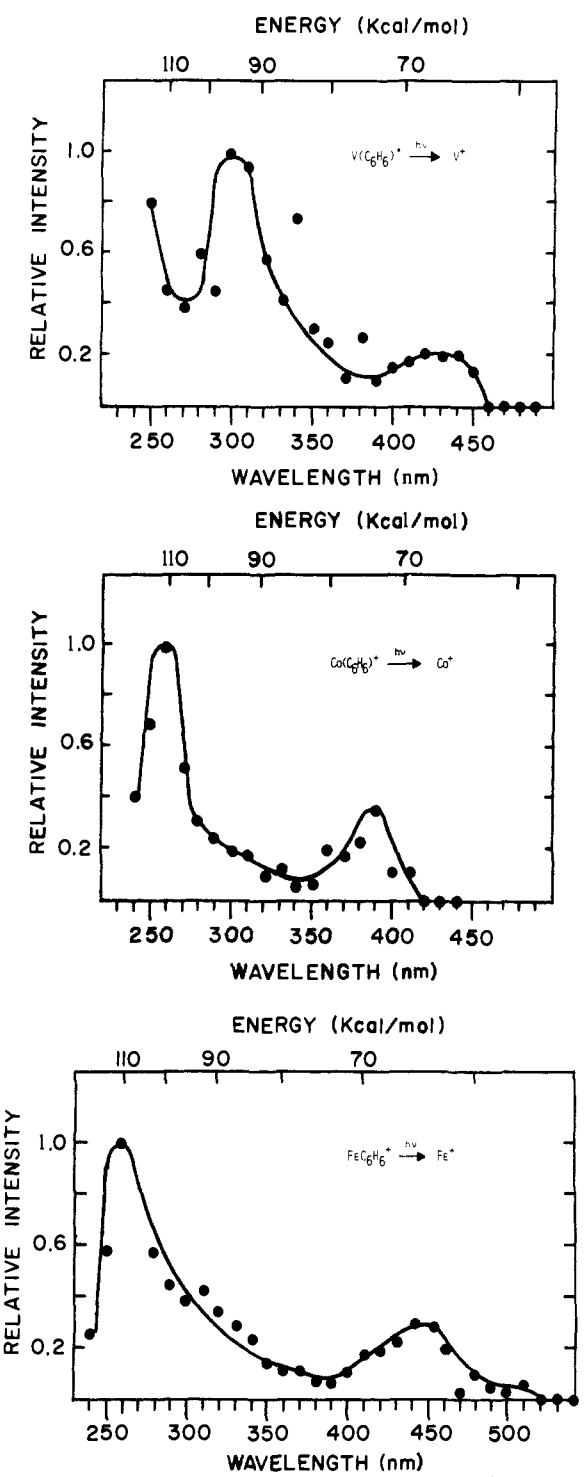

Figure 5. (a) The photodissociation spectrum of $VC_6H_6^+$ obtained by monitoring the appearance of V^+ as a function of wavelength. (b) The photodissociation spectrum of $CoC_6H_6^+$ obtained by monitoring the appearance of Co^+ as a function of wavelength. (c) The photodissociation spectrum of $FeC_6H_6^+$ obtained by monitoring the appearance of Fe^+ as a function of wavelength.

The photodissociation spectra of $CoC_6H_6^+$ and $FeC_6H_6^+$ are shown in Figure 5, b and c. For $CoC_6H_6^+$, a peak maximum is observed at 260 nm (σ = 0.02 Å^2), and the photodissociation threshold at 420 ± 10 nm yields $D°(Co^+–C_6H_6)$ = 68 ± 5 kcal/mol, which is in good agreement with other experimentally determined values.[33] For $FeC_6H_6^+$, peak maxima are observed at 260 nm (σ = 0.03 Å^2) and 440 nm. For comparison, an optical absorption spectrum obtained from the cocondensation of Fe vapor and benzene in an argon matrix at 170 K shows major peaks at 298 and 424 nm.[34] A threshold at 520 ± 20 nm implies $D°(Fe^+–C_6H_6)$ = 55 ± 5 kcal/mol. This value is somewhat lower than $D°(Fe^+–C_6H_6)$ = 59 ± 5 kcal/mol reported earlier, which was referenced as being approximately equal to $D°(Fe^+–H)$ = 58 ± 5 kcal/mol.[35] A more recent determination of $D°(Fe^+–H)$ = 47 ± 4 kcal/mol,[36] however, does suggest that a somewhat lower

(33) Jacobson, D. B.; Freiser, B. S. *J. Am. Chem. Soc.* **1984**, *106*, 4623.

(34) Morand, P. D.; Francis, C. G. *Organometallics* **1985**, *4*, 1653.
(35) Jacobson, D. B.; Freiser, B. S. *J. Am. Chem. Soc.* **1984**, *106*, 3900.
(36) Elkind, J. L.; Armentrout, P. B. *Inorg. Chem.* **1986**, *25*, 1078.

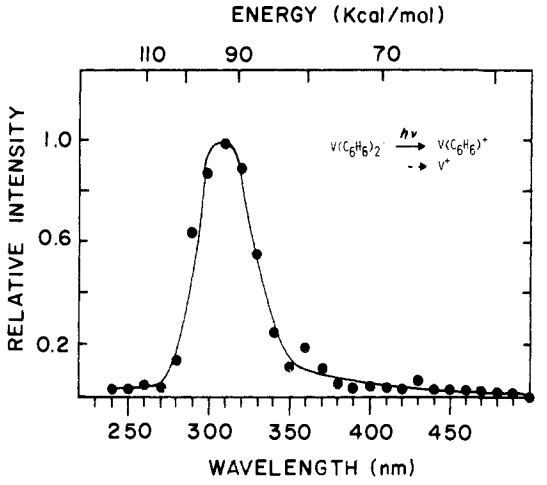

Figure 6. The photodissociation spectrum of $V(C_6H_6)_2^+$ obtained by monitoring the appearance of $VC_6H_6^+$ and V^+ as a function of wavelength.

value for $D°(Fe^+–C_6H_6)$ is likely.

The photodissociation spectrum of $V(C_6H_6)_2^+$ is shown in Figure 6. While a comparison with Figure 5a indicates that both $VC_6H_6^+$ and $V(C_6H_6)_2^+$ have about the same λ_{max}, the cross section for photodissociation of the bis-benzene complex is on the order of ten times larger, with $\sigma(310\text{ nm}) = 0.23$ Å^2. A dissociation threshold for $VC_6H_6^+$ formation from the bis-benzene complex is observed at 500 ± 20 nm, implying $D°(C_6H_6V^+–C_6H_6) = 57 \pm 5$ kcal/mol. This value is not different enough from $D°(V^+–C_6H_6)$ to suggest a synergistic effect. Continuous ejection of $VC_6H_6^+$ allows reaction 14 to be monitored. As expected, reaction 14 is not observed even at 250 nm, implying $D°(V^+–2C_6H_6) > 114$ kcal/mol.

$$V(C_6H_6)_2^+ + h\nu \rightarrow V^+ + 2C_6H_6 \qquad (14)$$

(F) MN^+. Heteronuclear transition metal cluster ions can be generated as shown in reaction 15.[33] The photodissociation spectrum of VFe^+ was the first reported for a bare heteronuclear

$$M^+ + Fe(CO)_5 \rightarrow MFe(CO)_x^+ \xrightarrow{CID} MFe^+ \qquad (15)$$

(M = any transition metal)

transition metal cluster ion[37] and revealed two peaks at 260 nm and 340 nm. The threshold at 380 nm yielded $D°(V^+–Fe) = 75 \pm 5$ kcal/mol, in good agreement with the results of ion–molecule reactions of VFe^+. This work has since been extended to include a variety of MFe^+ ions (where M is a 3d transition metal) and indicates that photodissociation will be a useful technique for obtaining spectroscopic and thermodynamic information on these cluster ions.[38]

(II) Isomer Differentiation. (A) $NiC_4H_8^+$. $NiC_4H_8^+$ ions were generated by reactions 16–19. Previous studies have indicated that each of these ions are distinct isomers.[39] The photodissociation

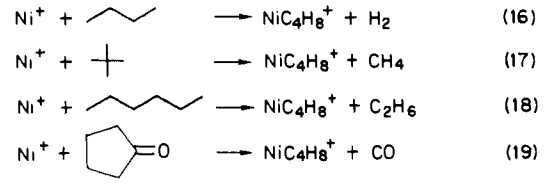

spectra of these ions are shown in Figure 7a–d. Table II compares the neutral losses for photodissociation (PDS) and collision-induced dissociation (CID) of these $NiC_4H_8^+$ ions.

The $NiC_4H_8^+$ ion produced in reaction 16 photodissociates to give two products of about equal intensity (loss of C_2H_4 and C_4H_8),

(37) Hettich, R. L.; Freiser, B. S. *J. Am. Chem. Soc.* **1985**, *107*, 6222.
(38) Hettich, R. L.; Freiser, B. S. *J. Am. Chem. Soc.*, submitted.

Table II. Comparison of Collision-Induced Dissociation vs. Photodissociation for $NiC_4H_8^+$ Isomers

structure	neutral losses CID[a]	neutral losses PDS
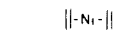	C_2H_4 C_4H_8	C_2H_4 C_4H_8
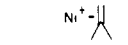	C_4H_8	C_4H_8 CH_4
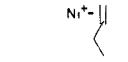	H_2 C_4H_8	H_2 C_4H_8 C_2H_4 CH_3
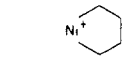	H_2 C_2H_4 C_4H_8	H_2 C_2H_4 C_4H_8

[a] Reference 39.

lending support to the fact that this ion is the bis-ethylene complex. CID and PDS reveal identical neutral losses for this ion. A cross-section $\sigma(310\text{ nm}) = 0.08$ Å^2 is obtained. Continuous ejection of $Ni^+–C_2H_4$ allows reaction 20 to be monitored. For wavelengths less than 360 nm, reaction 20 is observed, implying

$$\|–Ni^+–\| + h\nu \rightarrow Ni^+ + 2C_2H_4 \qquad (20)$$

$D°(Ni^+–2C_2H_4) = 80 \pm 5$ kcal/mol. The fact that this value is not significantly different than twice $D°(Ni^+–C_2H_4) = 37 \pm 2$ kcal/mol[8b] suggests that synergistic effects again are not very pronounced in this ion.

The ion produced in reaction 17 is assigned to be Ni^+–isobutene.[39] Collision-induced dissociation of this ion results in exclusive cleavage of C_4H_8 to form Ni^+. In addition to Ni^+, however, another photoproduct of about equal intensity, $Ni(C_3H_4)^+$, is also observed in the photodissociation of Ni^+–isobutene, reaction 21. No sharp cutoff is observed for reaction 21, which

occurs at wavelengths at least up to 450 nm. Three possibilities exist for $NiC_3H_4^+$: Ni^+–(allene), Ni^+–(cyclopropene), and Ni^+–(propyne). On the basis of thermodynamic data, either Ni^+–(allene) or Ni^+–(propyne) is the most likely structure.[31] Interestingly, Beauchamp and co-workers have observed using an ion beam instrument that Co^+ will react with isobutene in an endothermic reaction to produce $CoC_3H_4^+$ and CH_4.[40] The peak maximum for the photodissociation of Ni^+–isobutene is determined to be 280 nm ($\sigma = 0.03$ Å^2).

Ni^+–1-butene can be obtained by reacting Ni^+ with hexane, reaction 18.[39] Photodissociation of this species yields $NiC_4H_6^+$, Ni^+ (both observed in the CID of this ion), and $NiC_3H_5^+$ with a minor amount of $NiC_2H_4^+$ also observed. Monitoring the photoappearance of Ni^+ will not yield $D°(Ni^+–1\text{-butene})$ since any (or all) of the other three photoproducts may photodissociate to give Ni^+. Reaction 22 is observed to occur at wavelengths at

least up to 490 nm. Assuming $D°(Ni^+–\text{butene}) = 45 \pm 10$ kcal/mol,[41] this suggests a $D°(Ni^+–C_3H_5) < 60$ kcal/mol. Reaction 23 is observed,[42] implying $D°(Ni^+–C_3H_5) > 56$ kcal/mol.

$$NiD^+ + C_3H_8 \rightarrow Ni^+–C_3H_5 + H_2,HD \qquad (23)$$

(39) Jacobson, D. B.; Freiser, B. S. *J. Am. Chem. Soc.* **1983**, *105*, 736.
(40) Armentrout, P. B.; Halle, L. F.; Beauchamp, J. L. *J. Am. Chem. Soc.* **1981**, *103*, 6624.
(41) Bracketing techniques place the bond energy of 1-butene above ethylene and below butadiene, implying $D°(Ni^+–\text{butadiene}) = 45–60$ kcal/mol (estimated in ref 5b) > $D°(Ni^+–1\text{-butene})$ > $D°(Ni^+–\text{ethylene}) = 37 \pm 5$ kcal/mol (ref 8b).
(42) Carlin, T. J.; Sallans, L.; Cassady, C. J.; Jacobson, D. B.; Freiser, B. S. *J. Am. Chem. Soc.* **1983**, *105*, 6320.

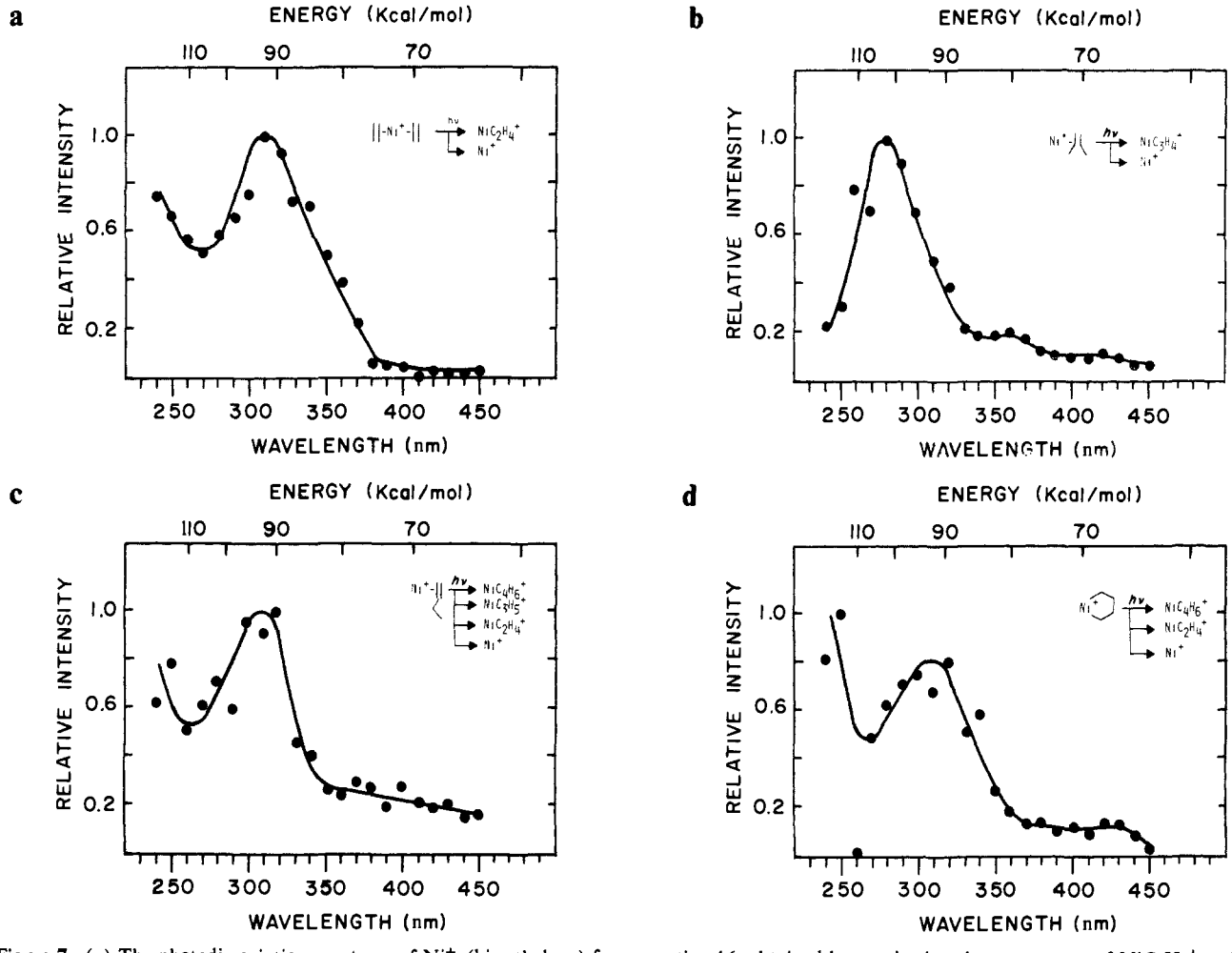

Figure 7. (a) The photodissociation spectrum of Ni^+–(bis-ethylene) from reaction 16, obtained by monitoring the appearance of $NiC_2H_4^+$ and Ni^+ as a function of wavelength. (b) The photodissociation spectrum of Ni^+–isobutene from reaction 17, obtained by monitoring the appearance of $NiC_3H_4^+$ and Ni^+ as a function of wavelength. (c) The photodissociation spectrum of Ni^+–(1-butene) from reaction 18, obtained by monitoring the appearance of $NiC_4H_6^+$, $NiC_3H_5^+$, $NiC_2H_4^+$, and Ni^+ as a function of wavelength. (d) The photodissociation spectrum of Ni^+–(metallocyclobutane) from reaction 19, obtained by monitoring the appearance of $NiC_4H_6^+$, $NiC_2H_4^+$, and Ni^+ as a function of wavelength.

These limits correspond well to a previously determined value of $D°(Ni^+–C_3H_5) \geq 55$ kcal/mol.[32] For comparison, $D°(Fe^+–C_3H_5) = 56 \pm 7$ kcal/mol.[43] The peak maximum for the photodissociation of Ni^+–butene is found to be 320 ± 10 nm ($\sigma = 0.05$ Å^2).

Reaction 19 is postulated to produce a metallocyclic $NiC_4H_8^+$ ion, structure I. Various studies, including ion–molecule reactions

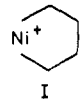

I

and collision-induced dissociation, have distinguished this ion from the bis-ethylene ion produced in reaction 16.[39,44] Surprisingly, photodissociation of the two $Ni^+–C_4H_8$ ions formed in reactions 16 and 19 is very similar, except H_2 elimination is observed for the ion from reaction 19. The predominant photoproduct from the metallocyclic ion is Ni^+ (loss of C_4H_8), and the peak maxima for this ion occur at 250 ± 10 and 320 ± 10 nm, with a cross section $\sigma(320\text{ nm}) = 0.12$ Å^2.

(B) $FeC_4H_6^+$. Two isomers of $FeC_4H_6^+$, Fe^+–butadiene and Fe^+–trimethylenemethane, are often postulated as the products of various dehydrogenation reactions. Fe^+–butadiene can easily be made by reaction of Fe^+ with 1-butene, reaction 24. Collision-induced dissociation of this ion results in exclusive cleavage of C_4H_6 to regenerate the metal ion. Photodissociation of Fe^+–butadiene produces Fe^+ as the only photoproduct. The photodissociation spectrum of this ion is shown in Figure 8a. A peak maximum is observed at 290 ± 10 nm, with a cross section $\sigma(290\text{ nm}) = 0.02$ Å^2. The photoappearance of Fe^+ is observed at wavelengths out to 590 ± 20 nm, implying $D°(Fe^+–\text{butadiene}) = 48 \pm 5$ kcal/mol. This is well within the previously estimated limits of $D°(Fe^+–\text{butadiene}) = 45–60$ kcal/mol.[43]

$$Fe^+ + \text{(1-butene)} \longrightarrow Fe^+(\text{butadiene}) + H_2 \qquad (24)$$

Electron impact ionization on (trimethylenemethane)iron tricarbonyl, process 25, generates several ions, including $FeC_4H_6^+$,

$$\text{(trimethylenemethane)}Fe(CO)_3 \xrightarrow{30\text{ eV}} Fe^+–C_4H_6 + 3CO \qquad (25)$$

which may be Fe^+–(trimethylenemethane). CID of this $FeC_4H_6^+$ species produces three products. At 77 eV translational energy, the product ratios are shown in reactions 26–28. In addition, reaction of this ion with 1-butene results in exclusive elimination

$$FeC_4H_6^+ \xrightarrow{31\%} FeC_2H_4^+ + C_2H_2 \qquad (26)$$
$$\xrightarrow{45\%} FeC_2H_2^+ + C_2H_4 \qquad (27)$$
$$\xrightarrow{24\%} Fe^+ + C_4H_6 \qquad (28)$$

of C_2H_4, reaction 29. These results indicate that the $Fe^+–C_4H_6$

$$FeC_4H_6^+ + \text{(1-butene)} \longrightarrow Fe(C_2H_2)(C_4H_8)^+ + C_2H_4 \qquad (29)$$

may have rearranged upon electron impact to yield an acetylene–ethylene complex, structure II. Attempts to generate and

II

(43) Jacobson, D. B.; Freiser, B. S. *J. Am. Chem. Soc.* **1983**, *105*, 7484.
(44) Halle, L. F.; Houriet, R.; Kappes, M.; Staley, R. H.; Beauchamp, J. L. *J. Am. Chem. Soc.* **1982**, *104*, 6293.

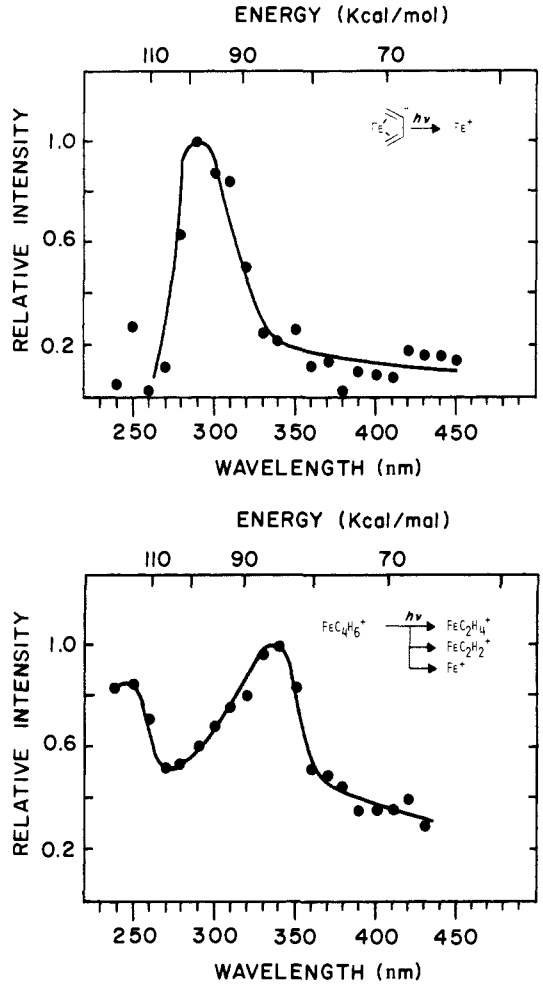

Figure 8. (a) The photodissociation spectrum of Fe^+–butadiene from reaction 24, obtained by monitoring the appearance of Fe^+ as a function of wavelength. (b) The photodissociation spectrum of Fe^+–C_4H_6 from reaction 25, obtained by monitoring the appearance of $FeC_2H_4^+$, $FeC_2H_2^+$, and Fe^+ as a function of wavelength.

isolate the ion having structure II by different reactions were unsuccessful. Photodissociation of the $FeC_4H_6^+$ ion from process 25 yields primarily $FeC_2H_2^+$ and Fe^+, with a minor amount of $FeC_2H_4^+$ also formed. The photodissociation spectrum is shown in Figure 8b. A peak maximum occurs at 340 ± 10 nm, giving $\sigma(340\text{ nm}) = 0.14$ Å^2. Continuous ejection of $FeC_2H_2^+$ and $FeC_2H_4^+$ allows reaction 30 to be monitored. The appearance

$$FeC_4H_6^+ + h\nu \rightarrow Fe^+ + C_4H_6 \qquad (30)$$

of Fe^+ from reaction 30 occurs at wavelengths up to 400 nm. This result indicates $D°(Fe^+–C_4H_6) > 72$ kcal/mol. If the $FeC_4H_6^+$ ion produced by process 25 existed as structure II, then $D°(Fe^+–C_4H_6) \sim D°(Fe^+–C_2H_4) + D°(Fe^+–C_2H_2)$, which must exceed 68 kcal/mol.[45] Thus, monitoring reaction 30 was insufficient in determining whether process 25 induced rearrangement of the $FeC_4H_6^+$ ion to structure II.

(III) Nature of Photodissociation. Many transition-metal ligand ions photodissociate in the ultraviolet and visible spectral regions, suggesting that these metal complexes have a high density of low-lying electronic states. Comparison of bond energies determined by photodissociation with those determined by other techniques shows good agreement, implying that dissociation thresholds observed in these spectra may be determined by thermodynamic and not spectroscopic factors. Clearly, however, a great deal of additional data must be obtained in order to determine the generality of this finding.

The maximum cross section for photodissociation varies considerably for these ions. One general trend observed is that the presence of two ligands on a metal ion produces a larger cross section than does one ligand. It is not evident why the cross sections for MCH_3^+ and FeS^+ are so much larger than the cross sections for $MC_6H_6^+$ and FeO^+. Preliminary investigations suggested that since the spectra of $FeOH^+$, $FeCO^+$, and $FeC_2H_4^+$ were very similar, except for thresholds, the absorption bands may be independent of the ligands.[17d] This assumption, while apparently true for these three complexes, appears to be the exception and not the rule. Interpretation of these spectra awaits detailed theoretical consideration.

Another exciting result of these studies is that different fragmentation is often observed for photodissociation compared to collision-induced dissociation. The reason for this difference, which may be due to the way the energy is added to the ion (e.g., vibrational vs. electronic excitation, stepwise vs. instantaneous),[46] is uncertain at this time. This notable difference makes photodissociation a powerful complementary tool to collision-induced dissociation for structural elucidation. In particular, collision-induced dissociation often suffers from the fact that ion rearrangement occurs prior to dissociation, obscuring the information desired. Photodissociation, on the other hand, is specific to the ionic structure at the time of photon absorption and may be more useful for distinguishing larger ions, where rearrangement is more predominant. Multiphoton infrared activation has also proved to be highly selective for organometallic isomer differentiation.[47] Dissociation by this technique in many cases occurs only via the lowest energy pathway, in contrast to the one-photon processes examined in this report. The fragmentation differences observed for these two techniques result because infrared excitation adds internal energy to an ion in its ground electronic state in a sequential, stepwise manner until the lowest energy activation barrier for dissociation is reached. In contrast, absorption of a single ultraviolet or visible photon produces an ion initially in an electronically excited state which may dissociate directly or, more likely, undergo rapid internal conversion to a vibrationally excited ground state leading to dissociation.

Acknowledgment is made to the Division of Chemical Sciences in the Office of Basic Energy Sciences in the United States Department of Energy (DE-AC02-80ER10689) for supporting this research and to the National Science Foundation (CHE-8310039) for continued support of the FTMS. R.L.H. would like to thank the W. R. Grace Co. for providing fellowship support.

Registry No. $FeCH_2^+$, 90143-30-9; $CoCH_2^+$, 76792-07-9; $FeCH_3^+$, 90143-29-6; $CoCH_3^+$, 76792-06-8; FeO^+, 12434-84-3; FeS^+, 60173-22-0; CoS^+, 102307-48-2; $V(C_6H_6)^+$, 102307-49-3; $Co(C_6H_6)^+$, 102307-50-6; $Fe(C_6H_6)^+$, 102307-51-7; $V(C_6H_6)_2^+$, 37298-48-9; VFe^+, 98330-71-3; Ni^+-$(C_2H_4)_2$, 83984-52-5; Ni^+-isobutene, 83984-55-8; Ni^+-$(CH_2)_4$, 83984-54-7; Ni^+-1-butene, 83984-53-6; Fe^+-butadiene, 102307-52-8; Fe^+-(trimethylenemethane), 102307-53-9.

(45) Acetylene will displace ethylene from Fe^+–C_2H_4, implying $D°(Fe^+–C_2H_2) > D°(Fe^+–C_2H_4) = 34 \pm 2$ kcal/mol (see ref 8b).

(46) Franchetti, V.; Freiser, B. S.; Cooks, R. G. *Org. Mass Spectrom.* **1978**, *13*, 106.
(47) Hanratty, M. A.; Paulsen, C. M.; Beauchamp, J. L. *J. Am. Chem. Soc.* **1985**, *107*, 5074.